Two-Dimensional Crystallization of Phthalocyanine Pigments at the Air/Water Interface

Brian W. Gregory,[†,‡] David Vaknin,[*,§] John D. Gray,[§] Benjamin M. Ocko,[||] Therese M. Cotton,[†] and Walter S. Struve[†]

Ames Laboratory-USDOE, Department of Chemistry, and Department of Physics and Astronomy, Iowa State University, Ames, Iowa 50011, and Department of Physics, Brookhaven National Laboratory, Upton, New York 11973

Received: September 3, 1998

Two-dimensional crystallization of highly planar phthalocyanine (Pc) pigments underneath the headgroups of a lipid Langmuir monolayer was observed and characterized by synchrotron X-ray diffraction at grazing angles of incidence (GID). The crystallization was achieved through spontaneous adsorption of positively charged, water-soluble Pc's to a spread dihexadecyl phosphate (DHDP) monolayer at the air/water interface. Analysis of the GID and rod profiles show that the lipid, pigment, and counterions form a complex in which the pigment plane is tilted with respect to the liquid surface; this is consistent with previous independent X-ray reflectivity investigations. In addition, the two-dimensional crystalline order of DHDP monolayers on pure H_2O has been determined and an analysis of its structure both before and after complexation is presented.

Introduction

The synthesis of novel crystalline molecular materials with tailored physical and electronic properties has increasingly been directed toward the use of organic molecular templates upon which nucleation can be achieved. In this regard, strategies for engineering organic crystals at a molecular level are quite versatile since they can utilize the wide diversity of intermolecular interactions that are present in molecular systems (e.g., van der Waals forces, hydrogen bonding, electrostatic interactions, charge-transfer mechanisms, etc.).[1,2] The use of organized lipid membrane architectures (e.g., bilayer vesicles, Langmuir monolayers, self-assembled films[2−6]) as templates for crystal growth is of great importance in both understanding and mimicking organic and inorganic natural biocrystallization processes.[3] Nevertheless, only recently has the application of such powerful structural characterization methods as in situ grazing incidence X-ray diffraction (GID) been employed to study the membrane/solution interface.[5] Langmuir monolayers at air/water interfaces provide a versatile framework from which such studies can be performed systematically, and recent investigations have probed the molecular arrangement of the interfacially confined, two-dimensional (2D) ordered aggregates that induce three-dimensional crystal nucleation from the subphase.[4] No evidence however has yet been reported concerning the *two-dimensional* crystallization of an organic species underneath such monolayers, which results in distinct reflections originating from the interfacial complex itself (as compared to the lipid framework). The work reported herein describes the 2D crystal structure of a water-soluble tetraazaphthalocyanine (AzPc) monolayer film Coulombically bound to the headgroups of a lipid Langmuir monolayer, as determined from in situ GID experiments performed directly at the air/water interface. This study differs from and complements the prior biocrystallization[3,4] work in two important respects. In addition to the characteristic diffraction from the hydrocarbon chain region of the lipid (although somewhat modified in width due to its interaction with the pigment), evidence for 2D crystallization of the lipid/AzPc complex itself is observed. Furthermore, in the present study, dilute micromolar (μM) subphase concentrations of AzPc are used, whereas supersaturated solutions are often used to induce 3D crystal growth at these interfaces.[3−5] The unique ability of the AzPc to form a closely packed, crystalline monolayer at the lipid headgroup/solution interface is dictated by its 4-fold symmetry and by both its attractive interactions with the lipid headgroups and repulsive interactions with neighboring phthalocyanines.

Phthalocyanines, the colorants of many inks, paints, plastics, and dyestuffs for cloths, are increasingly being used for various advanced technological applications.[7,8] This interest has arisen not only from their unique optical properties but also from their exceptional stability toward extreme environmental conditions (e.g., heat, acids, bases). They are notoriously insoluble in water and most organic solvents, making them very difficult to work with, but are appreciably soluble in concentrated acids and specialty solvents such as 1-chloronaphthalene. Only a few aqueous-soluble Pc's are commercially available, all of which are derivatized with ionizable sidegroups (such as SO_3^-) to effect their solubility. In the solid state, Pc's crystallize in a variety of polymorphic forms, most of which are generally characterized by stacking of the nearly planar macrocycles in linear columns.[7,8] Such *columnar* stacking is the result of strong van der Waals forces between the Pc planes, and it is this phenomenon that invariably leads to difficulties in controlling their aggregation state both in solution and in other condensed phases. Consequently, exciton splitting effects are observed in the electronic absorption spectra of dimers and higher order aggregates and are sensitive indicators of the nature of the species.[7−10] Such association problems are limited not only to Pc's but occur for other large macrocyclic systems (e.g., porphyrins, etc.) as well.

* To whom correspondence should be addressed.
† Ames Laboratory-USDOE and Department of Chemistry, Iowa State University.
‡ Present address: Department of Chemistry, Illinois State University, Normal, IL 61790-4160.
§ Ames Laboratory-USDOE and Department of Physics and Astronomy, Iowa State University.
|| Brookhaven National Laboratory.

10.1021/jp9836022 CCC: $18.00 © 1999 American Chemical Society
Published on Web 12/31/1998

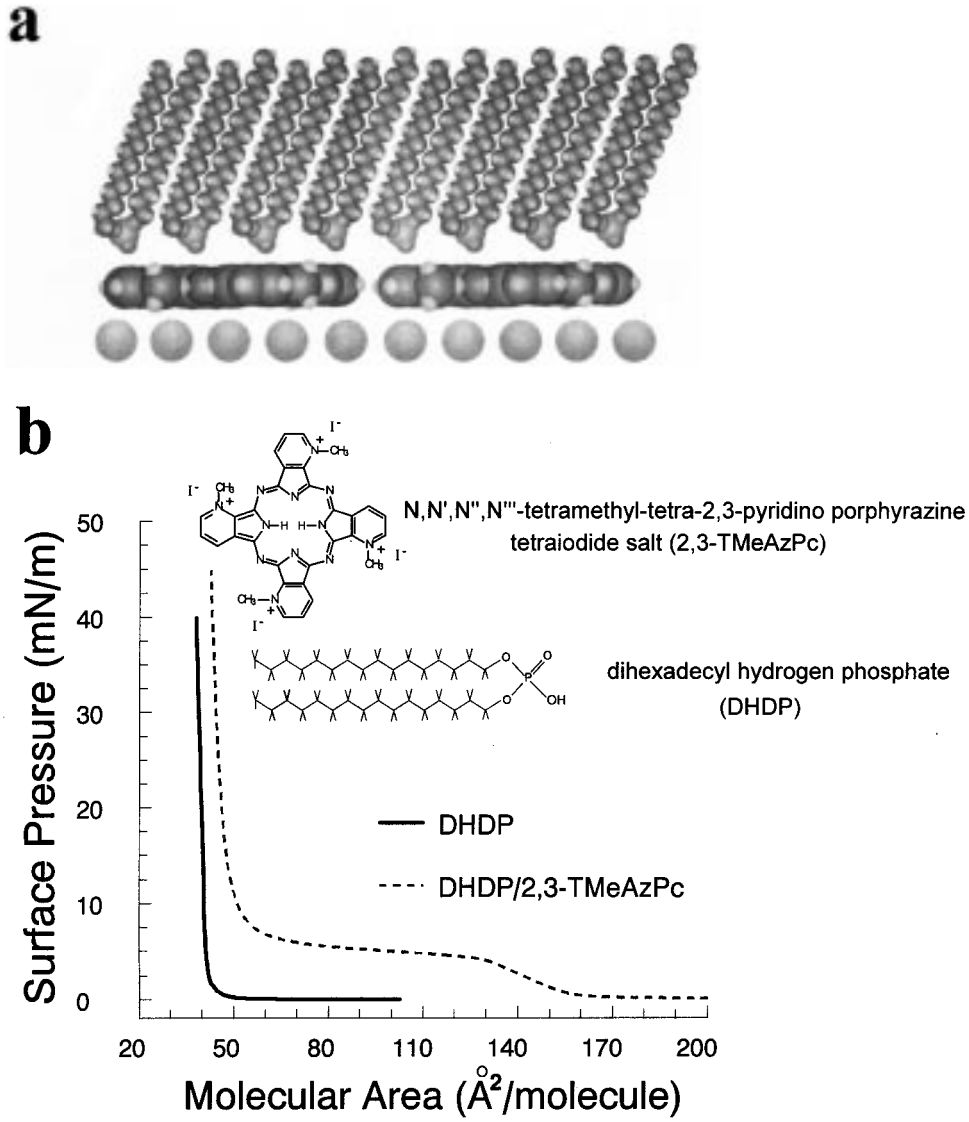

Figure 1. Illustration of (a) molecular organization of DHDP/2,3-TMeAzPc/I^- monolayer films at the air/water interface and (b) the compounds used in this work and surface pressure versus molecular area ($\pi-A$) isotherm of DHDP on water (solid line) and on 1 μM 2,3-TMeAzPc solution (dashed line).

As a means of studying and controlling these characteristics, Langmuir and Langmuir−Blodgett (L−B) monolayer techniques have been used extensively to form ordered molecular assemblies of Pc's[11−15] and porphyrins.[16,17] Nearly all of these investigations have involved pigments prederivatized with long alkyl chains (so as to introduce amphiphilic character to the film); yet despite the excellent film-forming properties of many of these derivatives, evidence indicates that none of these approaches has been able to eliminate their strong cofacial interactions. A more novel approach toward the formation of organized dye assemblies has been through an interfacial complexation route by which charged, water-soluble pigments are Coulombically associated at the air/water interface with a lipid Langmuir monolayer film containing oppositely charged headgroups (Figure 1a). This method has been used effectively to bind water-soluble phthalocyanines,[18−20] porphyrins,[18−22] and cyanine dyes.[23−31]

In previous reports,[18,19] the construction of unique artificial photosynthetic light-harvesting antenna assemblies using this interfacial complexation route and their subsequent structural characterization were described. These monolayer films were formed at the air/water interface by reaction of a spread Langmuir film of dihexadecyl hydrogen phosphate (DHDP) (Figure 1b) with a tetracationic phthalocyanine (*N*,*N*′,*N*″,*N*‴-tetramethyl-tetra-2,3-pyridino porphyrazine, tetraiodide salt; 2,3-TMeAzPc) (Figure 1b) dissolved in the aqueous subphase. The rationalization for selecting phthalocyanines as the preferred antenna pigments has been outlined previously,[18] and this particular methylated azaphthalocyanine was well-suited for these studies. Reasonably soluble in water, 2,3-TMeAzPc exhibits an aqueous optical absorption spectrum indicative of monomeric pigment species.[18,32] Monolayer surface pressure−molecular area ($\pi-A$) isotherms of DHDP on 1 μM 2,3-TMeAzPc aqueous subphases exhibited significant differences in comparison to those on pure H_2O (Figure 1b).[18] The limiting molecular area for DHDP at high surface pressures (>40 mN/m) increased from 41 ± 1 Å^2/molecule on pure H_2O to 46 ± 2 Å^2/molecule on the 2,3-TMeAzPc-containing subphases, indicating that the lipid films were expanded due to their interaction with interfacially bound pigments. In addition, the presence of a large plateau region in the $\pi-A$ isotherm for DHDP on the 2,3-TMeAzPc-containing subphases also demonstrated that interactions between the two components must be occurring at the interface.[18] A significant result from this work was the observation that visible absorption spectra of DHDP/2,3-TMeAzPc LB monolayers were virtually identical in both band

positions and line widths to that of the monomer in solution,[18,32] indicating the formation of a closely packed single pigment layer whose aggregation tendencies were almost completely suppressed. As described previously,[18] the need to eliminate spontaneous pigment aggregation while maintaining high pigment surface densities is one very crucial factor in the design of efficient antenna complexes.

X-ray reflectivity measurements performed on the complexed DHDP/2,3-TMeAzPc monolayer[18] indicated the presence of a closely packed single pigment layer contiguous to the lipid headgroups and a hydration sphere within the headgroup/pigment region (with the possible formation of an iodide counterion layer beneath the AzPc layer (Figure 1a)). From the combined X-ray and optical absorption results,[18] it appeared that the natural tendency for these pigments to self-aggregate in the complexed state at the air/water interface was overridden both by the attractive Coulomb interactions with the DHDP headgroups (which effectively bind the pigment to the monolayer) and by the strong repulsive Coulomb interactions between neighboring macrocycles. Those results combined with the 2D GID structural study presented below yield a more complete picture of interfacial organization in these complexed monolayers. In addition, the 2D crystalline order of DHDP monolayers on pure H_2O has been determined and an analysis of its structure both before and after complexation is presented.

Experimental Section

Experiments were performed on the Harvard−Brookhaven liquid-surface X-ray spectrometer (X22B beamline) at the National Synchrotron Light Source (NSLS) at Brookhaven National Laboratory; the NSLS spectrometer (operating at $\lambda = 1.583$ Å) has been described previously.[33] A thermostated Langmuir trough equipped with a Wilhelmy surface pressure sensor, and contained within a gas-purgeable enclosure was installed on the diffractometer. The enclosure was purged with He during experiments in order to reduce incoherent background scattering from air and reduce radiation damage. Details concerning the materials involved and monolayer preparation were described previously.[18,19] In the GID experimental configuration, a monochromatic X-ray beam is incident at angles that are slightly below the critical angle ($\alpha_i \approx 0.8\alpha_c$; $\alpha_c = 0.157°$) in order to minimize scattering from the bulk subphase. At these angles, total external reflection occurs, which effectively limits the penetration depth of the X-ray beam to that of the evanescent wave.[34] Fulfillment of the Bragg diffraction condition for a 2D crystalline monolayer at the interface with a 2D reciprocal lattice vector $\boldsymbol{\tau}_\perp$ requires that $Q_\perp - \boldsymbol{\tau}_\perp = 0$, where $Q_\perp$ is the component of the scattering vector in the horizontal plane. In an ideal 2D system, the vertical component of the scattering vector Q_z has no restriction and therefore Bragg scattering will extend in reciprocal space along a direction orthogonal to the interface (i.e., parallel to Q_z); such variations of scattering intensity along the surface normal are called *Bragg rods*.[34,35] As a result of the finite thickness of the film, the rod profile is governed by the vertical component of the form factor of the Bragg reflecting objects. Whereas the *rod* profile provides information on the electron density across the interface from the crystalline portion of the film, the specular reflectivity is obtained as an average over the entire portion of the film, including domain boundaries and imperfections, regardless of crystallinity.

Results and Discussion

1. DHDP on Pure H_2O. GID measurements on spread films of DHDP on H_2O were performed in the range 0.15 Å$^{-1} \leq Q_\perp \leq 1.75$ Å^{-1} at temperature $T = 18$ °C as a function of surface pressure π. The appearance of a single low-order diffraction peak was observed to occur during film compression, which appeared to shift position during that time in accordance with a decrease in lattice spacing (see below). The presence of such a single reflection over most of the compression/decompression cycle indicates the following: (1) a single repeat distance d_{hk} and hence hexagonally symmetric hydrocarbon chain packing within the film and that this arrangement is relatively unaffected by the compression process; (2) a vertical orientation of the dialkyl phosphate at the interface, since tilting of the hydrocarbon chains either along nearest neighbor (NN) or next-nearest neighbor (NNN) directions within the lattice would produce distortions of the unit cell, leading to multiple reflections. This portrait of interfacial orientation for DHDP monolayers is also consistent with experimental Bragg rod profiles discussed below.

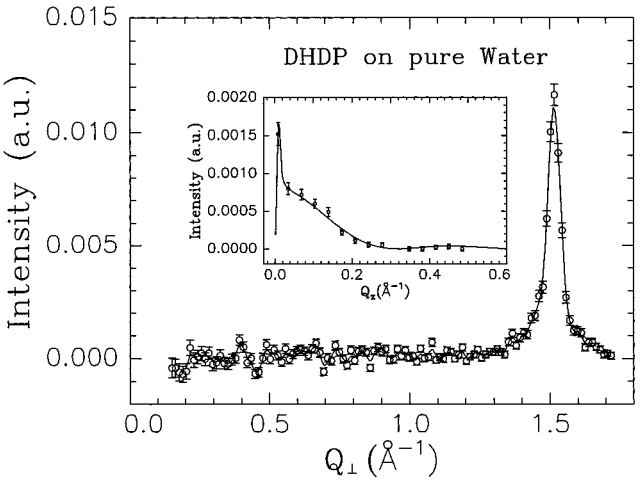

Figure 2. $Q_\perp$ scan and Q_z-resolved rod profile (inset) at the $(1,\bar{1})$ Bragg reflection ($Q_\perp = 1.516$ Å^{-1}) for DHDP on H_2O ($\pi = 20.8$ mN/m), with a *diffraction-derived* molecular area ($A_{DHDP} = 4d/\sqrt{3}$) $A_{DHDP} = 39.66$ Å^2/molecule.

Figure 2 displays both the $Q_\perp$ scan and the Q_z-resolved rod scan (inset) for DHDP at $\pi = 20.8$ mN/m. The low-order reflection measured at $Q_\perp = 1.516$ Å^{-1} corresponds to hexagonally ordered single hydrocarbon chains with a spacing $d = 4.144$ Å.[35] This yields a chain cross-sectional area of $A_{chain} = 19.83$ Å^2, and thus the *diffraction-derived* molecular area for DHDP is given by $A_{DHDP} = 2A_{chain} = 39.66$ Å^2/molecule since the phosphate headgroup cross-sectional area is smaller than that for the two alkyl chains.[18] The Bragg rod profile (Figure 2, inset) obtained at the same π shows that the scattering intensity has a maximum at $Q_z \approx 0$ Å^{-1}, indicating that DHDP has a near vertical orientation at the interface.[35] This agrees well with the conclusion from the *reflectivity-derived* molecular tilt angles ($t = 7° \pm 7°$)[18,19] and from the fact that only a single Bragg reflection is observed even at finite Q_z values (not shown). The rod profile exhibits a width (fwhm) of 0.278 Å^{-1} from which the molecular length can be estimated by $l = 5.56/(\Delta Q_z \cos t)$ (where ΔQ_z denotes the fwhm of the bell-shaped curve and t is the tilt angle[5]). Assuming $t = 0°$, substitution yields $l = 20.0$ Å, which corresponds to the approximate length of the hydrocarbon chain portion of the molecule. This is in agreement with previous X-ray reflectivity results ($l = 19.7 \pm 0.4$ Å).[18] In more quantitative terms, the variation in intensity $I(Q_z)$ along the rod is related to the molecular structure factor $F(Q_\perp,Q_z)$ through the relation[34,35]

$$I(Q_z) \approx |t^i(k_z^i)|^2 |F(Q_\perp,Q_z)|^2 e^{-(Q_z\sigma)^2} |t^f(k_z^f)|^2 \qquad (1)$$

where $t^i(k_z^i)$ and $t^f(k_z^f)$ are the initial and final Fresnel transmission functions that account for multiple scattering (in the distorted wave Born approximation) between the air/water interface and the film.[5] The exponential term includes a Debye−Waller-like factor, which accounts for vertical roughness at the interface due to capillary waves and intrinsic surface imperfections. For simple linear molecules, the structure factor can be separated into two components, one along (Q_z) and one orthogonal ($Q_\perp$) to the molecular axis,[34,35] such that $F(Q_\perp,Q_z) = F_\perp(Q_\perp)F_z(Q_z)$. In the molecular frame (denoted by a prime), the Q_z' component is represented as the Fourier transform of a one-dimensional aperture of length l[35]

$$F_z(Q_z') = (\sin u)/u \tag{2}$$

where $u = (Q_z'l)/2$. If the molecule tilts with respect to the surface normal, a transformation of eq 2 from the molecular coordinates to one relative to the liquid surface is required and is given by (assuming tilt toward the in-plane scattering vector)[35]

$$\begin{aligned} Q_x' &= Q_x \cos t + Q_z \sin t \\ Q_y' &= Q_y \\ Q_z' &= -Q_x \sin t + Q_z \cos t \end{aligned} \tag{3}$$

As a result of the hexagonal symmetry of the lattice, there are six equivalent domains nominally with the same tilt angle, however having six inequivalent tilt directions with respect to the scattering vector direction (defined in eq 3 as the x-axis). The variation of $F(Q_\perp)$ for a linear molecule is negligible for small tilt angles (≤30°) and therefore can be approximated by a constant.[5] In fitting the data to eq 1, two models with chain tilt toward NN and to NNN were examined using three independent parameters: an overall scale factor, the molecular length (l), and the tilt angle (t). The analysis yielded $l = 19.7$ Å and $t \approx 0.0°$, which is in agreement with the reflectivity results.[18]

Shifts in the $Q_\perp$ position of the observed $(1,\bar{1})$ reflection are presented in Figure 3 at the various surface pressures upon decompression. The incremental changes in the diffraction-derived molecular areas correspond well with those obtained from the isotherms in this region. In this pressure range (0.8−21 mN/m, $A_{DHDP} \approx 41-44$ Å^2), the reversibility of the isotherms was evidenced by the observation of similar diffraction patterns upon compression (data not shown). Upon decompressing the monolayer to larger molecular areas ($A_{DHDP} \geq 45$ Å^2, $\pi \approx 0$ mN/m), residual $(1,\bar{1})$ Bragg reflections were observed indicating the coexistence of well-ordered regions within the fluid phase.[36]

2. DHDP on 2,3-TMeAzPc-Containing Aqueous Subphases. Spread films of DHDP on 1 μM 2,3-TMeAzPc aqueous subphases at 18 °C yielded two low-order Bragg reflections in the range 0.15 Å$^{-1} \leq Q_\perp \leq$ 1.75 Å^{-1} upon compression (Figure 4a). One of these reflections corresponds to diffraction from the organized hydrocarbon chain region ($Q_\perp = 1.482$ Å^{-1}) with noticeable differences in peak positions, widths, and intensities in comparison with the corresponding Bragg reflection from the lipid monolayer spread on pure H_2O at similar lateral pressures ($Q_\perp = 1.521$ Å^{-1}) (Figure 5).[37] Quantitatively, there is a small increase in alkyl lattice spacing d (hexagonal lattice) on the 2,3-TMeAzPc-containing subphase ($d = 4.240$ Å on Pc solution compared to $d = 4.131$ Å on pure H_2O), indicating that the hydrocarbon tails still exist within a closely packed environment even when complexed by the pigment.[35] The difference in the d spacing corresponds to a slight increase in the *diffraction-derived* molecular area ($A_{DHDP} = 4d/\sqrt{3}$) from $A_{DHDP} = 39.4$ Å^2/molecule on H_2O to $A_{DHDP} = 41.5$ Å^2/molecule on 1 μM 2,3-TMeAzPc. This increase in molecular area is consistent with the increase in the limiting molecular area observed in the pressure vs molecular area ($\pi-A$) isotherm: 42.0 Å^2/molecule on pure H_2O compared to 45.0 Å^2/molecule on the pigment solution (Figure 1b). (It should be noted that the *diffraction-derived* molecular area does not necessarily reflect the one extracted from the isotherms, because the former does not include imperfections and zone boundaries between domains, whereas the latter is averaged over the whole surface.) Consequently, the constraint of maintaining closely packed alkyl tails in the midst of an increase in molecular area requires that the lipid molecules tilt away from the surface normal on these pigment-containing subphases. Such a picture of lipid organization in these complexed monolayers is in full agreement with the reflectivity results and therefore strongly supports the interfacial model used to fit the experimental reflectivities. As demonstrated below, it is the *entire* complex, including the pigment plane and the lipids, which tilts as a rigid unit with respect to the liquid surface.

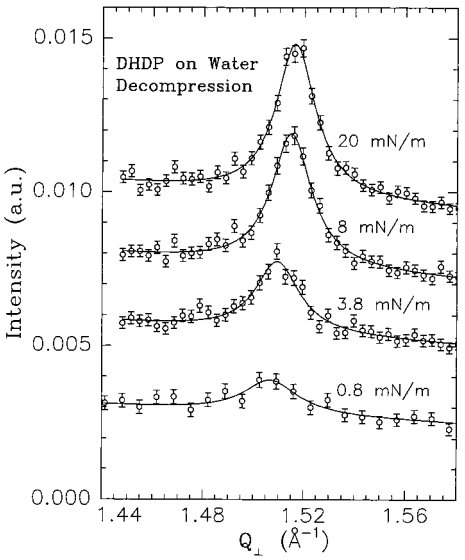

Figure 3. The $(1,\bar{1})$ Bragg reflection of DHDP on pure water at various surface pressures upon decompression, demonstrating an increase in molecular area and loss of long-range order. The *diffraction-derived* molecular area as the monolayer is decompressed is $A_{DHDP} = 39.66$ Å^2/molecule ($\pi = 20.8$ mN/m), $A_{DHDP} = 39.73$ Å^2/molecule ($\pi = 8$ mN/m), $A_{DHDP} = 40.02$ Å^2/molecule ($\pi = 3.8$ mN/m), and $A_{DHDP} = 40.16$ Å^2/molecule ($\pi = 0.8$ mN/m). Similar results were obtained from the initial compression, revealing reversibility in the film structure upon cycling.

The position of the second reflection (Figure 4b) was found to be strongly dependent on surface pressure; peak position values at $Q_\perp = 0.238$ Å^{-1} and $Q_\perp = 0.215$ Å^{-1} were obtained at $\pi = 35$ mN/m and $\pi = 13$ mN/m, respectively. These values correspond to a variation of $d_{complex}$ spacing in the range of (26.4−29.2) ± 0.2 Å. This is nearly twice the edge length expected for 2,3-TMeAzPc based on known lattice spacings of similar unsubstituted phthalocyanines obtained from bulk crystal structure X-ray diffraction analysis[38,39] and unit cell spacings for phthalocyanine monolayer films on both metal[40,41] and metal dichalcogenide surfaces.[9,10,42] No splitting of the reflection was observed at any finite Q_z as the surface pressure was varied. Similar variations in Bragg reflection peak positions of fatty acid monolayers at the air/water interface have been observed and associated with the continuous tilt of the hydrocarbon chains from the surface normal. Such tilts usually give rise to a splitting

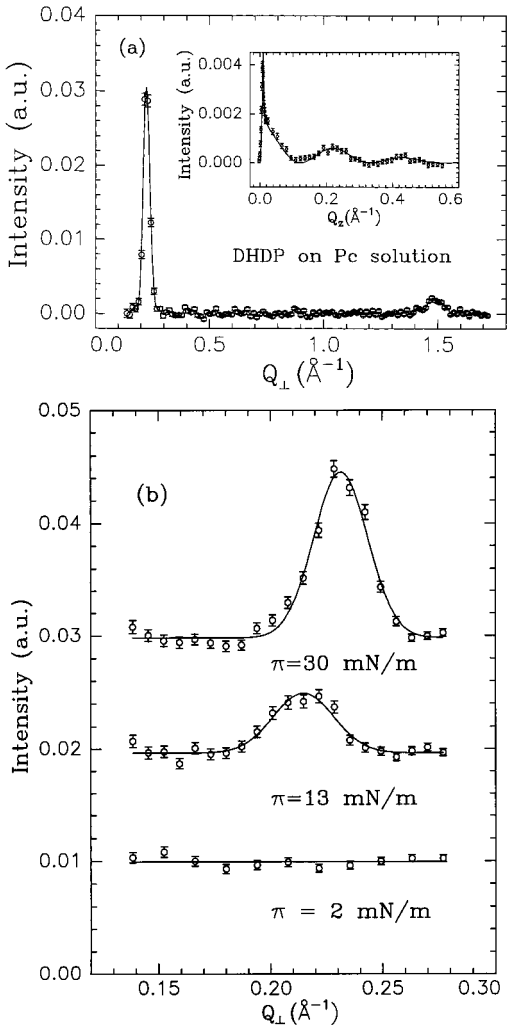

Figure 4. (a) Intensity versus $Q_\perp$ scan for DHDP on 1 μM 2,3-TMeAzPc ($\pi = 25$ mN/m), showing two Bragg reflections: one due to the ordering of the lipid chains ($Q_\perp \cong 1.48$ Å^{-1}, $A_{DHDP} = 41.51$ Å^2/molecule) and the other at low $Q_\perp$ values due to the crystallization of the pigment−lipid complex ($Q_\perp = 0.226$ Å^{-1}). This peak is associated with the (11) or the equivalent (1,$\bar{1}$). The insert shows a rod scan along Q_z at the Bragg reflection ($Q_\perp = 0.226$ Å^{-1}). The solid line in the inset is calculated from a model as described in the text. (b) Bragg reflection associated with the ordering of the DHDP/AzPc complex at various surface pressures (with corresponding *isotherm-derived* molecular areas $A_{DHDP} = 41.51$, 50.0, and 107.0 Å^2/molecule). The peak position and intensity is highly sensitive to the surface pressure in the film.

of the low-order hexagonal reflection due to the broken hexagonal symmetry.[5,34,35] The continuous variation in peak position associated with the complex, in conjunction with no apparent peak splitting, indicates an isotropic deformation of a highly symmetric unit cell, i.e., a square or hexagonal lattice. In accordance with these constraints, we propose a model of the interfacial molecular organization.

2.1. Lipid/Pc Complex Tilting Model. In the lipid/Pc tilting model, the in-plane ordering of the complex can be derived by slight distortion of the square lattice naturally formed by the pigments. As shown in Figure 6a, we propose that each pigment (depicted by a square tile) is tilted over one of its diagonals by a tilt angle t in an orderly manner that yields to a first approximation a $\sqrt{2} \times \sqrt{2}$ superlattice. This model, with a tilted complex along one of the diagonals, yields a distortion of the $\sqrt{2} \times \sqrt{2}$ superlattice, creating a centered rectangular lattice with two complexes per unit cell. The lowest order Bragg

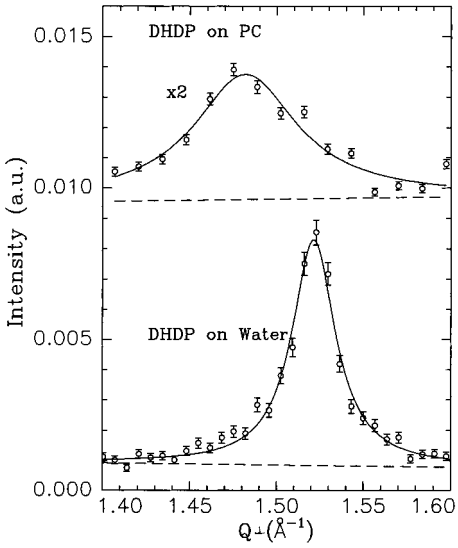

Figure 5. Bragg reflections associated with the hexagonally ordered hydrocarbon chains of DHDP on both a pure H_2O subphase ($\pi = 25$ mN/m, $A_{DHDP} = 39.4$ Å^2/molecule) and on a 1 μM 2,3-TMeAzPc solution ($\pi = 25$ mN/m, $A_{DHDP} = 41.51$ Å^2/molecule).

reflections of such a centered rectangular lattice, (10) and (01), have a very weak structure factor (in fact, if the two complexes in the unit cell are equivalent, the structure factor is exactly zero). As argued below, the observed peak is associated with the (11) and the equivalent (1,$\bar{1}$) Bragg reflections that exhibit a much stronger structure factor.

A side view of the staggered and tilted boxes along the diagonal is shown in Figure 6b, where adjacent staggered diagonals are tilted in opposite directions. This model strongly affects the calculated scattering along the *rod*, which can be used to examine the feasibility of our model. The inset in Figure 4a shows a scan along the *rod* of the Bragg reflection at $Q_\perp = 0.226$ Å^{-1} at $\pi = 25$ mN/m. In qualitative terms, the variation of the intensity along the *rod* indicates that the length of the scattering entities (i.e., normal to the interface) is $2\pi/\Delta Q_z \approx 30$ Å, where ΔQ_z is the separation between the two maxima in the rod scan. This length cannot be associated either with the lipid (total length of DHDP $\cong$ 23 Å) or the pigment by itself and most likely reflects the total length of the complex as derived from the reflectivity.[18] To analyze the *rod* scan in quantitative terms, the complex is assumed to have a boxlike shape with a square cross section (reflecting the square geometry of the Pc) of side length a and height l (Figure 6b). The structure factor of the complex together with multiple scattering effects due to the subphase[43] dominates the scattering along the rod. In terms of its principal axes, the structure factor of the boxlike entity is given by

$$F_{mol}(Q'_x,Q'_y,Q'_z) = \frac{\sin(u_x)}{u_x}\frac{\sin(u_y)}{u_y}\frac{\sin(u_z)}{u_z} \qquad (4)$$

where $u_x = Q'_x a/2$, $u_y = Q'_y a/2$, and $u_z = Q'_z l/2$. Tilting the boxes in unison with respect to the surface normal and the scattering vector (as described above) thus causes the distortion of the unit cell. Hence, the projection of the aperture onto a direction parallel to the tilt axis (i.e., x axis, Figure 6b) correlates with the experimental d_{hk} spacing. As in the case of simple alkyl chains (see section 1), this tilting requires a transformation of the molecular coordinates in eq 4 with respect to the scattering vector ($Q = (Q_\perp, Q_z)$).[35] In fitting the rod scan (assuming three independent parameters a, l, and tilt t), we have examined many models with tilts along other high-symmetry axes as well as other configurations and superlattices. Our best fit to the rod

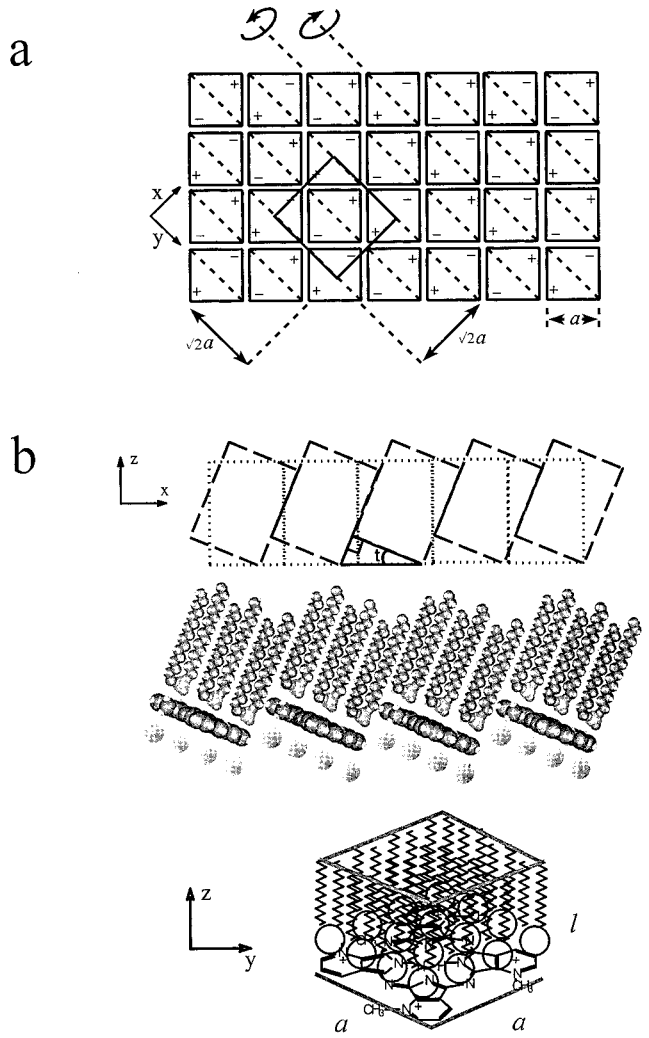

Figure 6. (a) Model structure of DHDP−Pc complex at the air/water interface. Squares represent the cross section of the complex with the (+) and (−) indicating whether a corner is above or below the plane, respectively. Tilting the boxes by an angle t along the diagonal (i.e., y axis) creates to a first approximation a $\sqrt{2} \times \sqrt{2}$ superlattice. This model, with a tilted complex along one of the diagonals, yields a distortion of the $\sqrt{2} \times \sqrt{2}$ superlattice, creating a centered rectangular lattice with two complexes per unit cell. The Bragg reflection at $Q_{\perp} = 0.226$ Å^{-1} displayed in Figure 2 is due to the (11) or the equivalent $(1,\bar{1})$ Bragg reflection from the superlattice. (b) A side view of the staggered *boxes* (representing the complexes) along the diagonal (viewed parallel to the x axis). Nearest neighbor diagonals are tilted in opposite directions. Each box-shaped complex has a square cross section (of dimension a^2) and height l, containing a single DHDP/2,3-TMeAzPc/I$^-$ complex. The iodide counterions have been omitted for clarity. The projection of the aperture onto the x axis yields the experimental spacing (i.e., $d_{\text{complex}} = a/\cos t$).

scan is most consistent with the peak at $Q_{\perp} = 0.226$ Å^{-1} associated with the (11) (or the equivalent $(1,\bar{1})$) Bragg reflection in terms of the $\sqrt{2} \times \sqrt{2}$ superlattice. A molecular-level interpretation of the extracted parameters from the fit reveals: (1) A DHDP/2,3-TMeAzPc/I$^-$ complex thickness (l) of 33.5 ± 2.5 Å, which correlates well with that obtained from corresponding specular X-ray reflectivity measurements (32.0 ± 0.7, ref 18); (2) A molecular complex tilt angle $t = 35 \pm 10°$ (relative to the surface normal, Figure 6b) (This also agrees with reflectivity-derived hydrocarbon tail tilt angles (30.8° ± 1.8°, ref 18) measured at similar lateral pressures. Since the hydrocarbon tilt is approximately the same as that of the complex, it is reasonable to conclude that the hydrocarbon chains are essentially perpendicular to the macrocycle plane (Figure 6b); (3) A molecular complex width $a = 22.0 \pm 2.0$ Å, yielding a d spacing of $d^{\text{rod}}_{\text{complex}} \approx a/\cos t = 27.2$ Å, which is consistent with the d spacing derived from the GID (for this particular pressure, $d_{\text{complex}} = 27.8$ Å). This value is larger than the side length of the pigment, suggesting that the complex possibly includes iodide counterions as well.

2.2. Pc Single-Layer vs Bilayer Model. Although the lipid/Pc tilting model assumes the complexation of a *single* AzPc layer beneath the lipid phosphate headgroups at the air/water interface, the formation of an AzPc bilayer cannot be ruled out from the present X-ray results alone. The notion of a single AzPc layer underneath the lipid was previously justified from the electronic absorption spectra of transferred monolayer films, which demonstrated the presence of a single pigment layer.[18] However, Martín and Möbius[44,45] have suggested recently that with similar lipid/pigment films one cannot necessarily infer that the film arrangement at the air/water interface mirrors that after transfer onto solid support. These authors have proposed the existence of a surface pressure-dependent monomer/dimer equilibrium in a related system involving the complexation of 5,10,15,20-tetrakis(1-methyl-4-pyridyl)-21H,23H-porphine (TMePyP) with a dimyristoylphosphatidic acid (DMPA) Langmuir monolayer.[44,45] In their model, both monomers and dimers lie parallel with the interfacial plane; the dimer phase consists of pigments that are stacked in a parallel arrangement and rotated by 45° with respect to each other. Their depiction of interfacial pigment organization was inferred from differences observed in the TMePyP electronic absorption spectra in its complexed state at the air/water interface compared to its monomeric spectrum in dilute organic solution. Furthermore, these authors demonstrated that the transferred monolayers on glass substrates consisted of TMePyP monomers only and proposed that only those pigments that are contiguous to the phospholipid headgroups are transferred during the LB process. It should be noted, however, that whereas complexation in the present study was attained by spreading the lipid on a dilute aqueous solution containing Pc,[18,19] these authors employ a cospreading method in which the phospholipid and pigment are combined at their expected optimal molar ratio in a spreading solvent and deposited directly at a pure H_2O surface. Such differences in protocol may invariably lead to significant differences in monolayer organization at the air−water interface.

In light of this depiction of interfacial pigment organization, alternative models based on the formation of AzPc dimers can be derived that may also explain the in-plane ordering of the complex. Clearly, these models must consist of a highly symmetric unit cell (i.e., a square lattice) that undergoes an isotropic deformation upon compression. In order for such a model to be reasonable, however, it must also be compatible with prior in situ reflectivity investigations of the DHDP/2,3-TMeAzPc system,[18,19] which are reexamined below. In these previous studies, the total electron density ρ (e$^-$/Å^3) contained within the portion of the three-dimensional interfacial "box" (of cross-sectional area $A_{\text{DHDP}}(\pi)$ and thickness d_{total} (in Å)) that contains the pigment was defined to be

$$\rho = (\tau N_{\text{e,pigment}} + N_{\text{H}_2\text{O,pigment}} N_{\text{e,H}_2\text{O}})/(A_{\text{DHDP}} d_{\text{pigment}}) \quad (6)$$

where τ is the fraction of pigment per lipid, $N_{\text{e,pigment}}$ and $N_{\text{e,H}_2\text{O}}$ are the number of electrons per pigment and H_2O (518 e$^-$ and 10 e$^-$, respectively), $N_{\text{H}_2\text{O,pigment}}$ is the number of water molecules associated with the pigment per lipid, and d_{pigment} is the thickness (in Å) of the pigment portion of the interfacial box.[18] (The values extracted from the fits for these variables were $\tau = 0.231 \pm 0.015$, $N_{\text{H}_2\text{O,pigment}} = 13.8 \pm 0.6$, and d_{pigment}

$= 12.5 \pm 0.2$ Å.[18]) On the basis of the absorption spectra of the transferred films (which might *not* reflect the actual in situ interfacial structure), the model assumed a single intact AzPc layer contiguous to the lipid headgroups; any electron density extracted from the modeling in excess of that expected for a single 2,3-TMeAzPc layer was partitioned into interfacial H_2O molecules (and/or iodide counterions). Since the chemical identities from which this excess originates are not known a priori, it is equally valid to assume that some (or all) of it arises from AzPc's, unless evidence indicates otherwise. In the extreme that the excess electron density arises not from interfacial water but solely from additional pigment, such an excess would equal $(13.8\ H_2O/\text{lipid})(10\ e^-/H_2O) = 138\ e^-/\text{lipid}$, equating to an extra 0.266 AzPc/lipid. Thus, the total electron density within the AzPc portion interfacial box would be equivalent to $(0.231 + 0.266) = 0.497$ AzPc/lipid and therefore would be consistent with a *completely intact 2,3-TMeAzPc bilayer*. However, neither of these possibilities (single/bilayer) can presently be ruled out since it is not known from whence the excess electron density arises nor how it is partitioned between interfacial H_2O and/or 2,3-TMeAzPc. In situ electronic absorption measurements similar to those conducted by Martín and Möbius may resolve the problem. Alternatively, neutron reflectivity measurements using isotope substitution of the subphase, as well as of the lipid, may shed light on the water content in the pigment region.

Summary

These studies represent evidence for the *two-dimensional crystallization* of water-soluble pigments underneath a Langmuir monolayer. GID experiments of dihexadecyl phosphate monolayers Coulombically complexed with water-soluble, positively charged azaphthalocyanines at the air/water interface evidence strong diffraction signals arising from both the alkyl tail region of the lipid and the lipid−pigment complex itself. The diffraction-derived molecular area per lipid obtained from the reflection arising from the alkyl tail region is consistent with highly organized alkyl chains. In comparison with that arising from the lipid on pure H_2O, the GID evidenced a slight expansion in the alkyl chain lattice spacing ($\Delta d = 0.10$ Å) in response to complexation of the lipid by the subphase-soluble pigment. Assuming the presence of a single AzPc layer at the interface, the second reflection (i.e., that of the complex) corresponds to a square lattice spanned by *boxlike* tilted complexes. The Bragg *rod* analysis of this reflection provides an independent test for the feasibility of our model. Models employing an AzPc bilayer however cannot be ruled out from the available X-ray data. Similar interfacial complexation and diffraction experiments were performed with the water-soluble cationic porphyrin TMePyP; however, no reflections were observed with those films, possibly for reasons that have been outlined previously.[18]

Acknowledgment. Iowa State University under Contract W-7405-Eng-82 operates The Ames Laboratory for the U.S. Department of Energy. This work was supported by the Division of Chemical Sciences, Office of Basic Energy Sciences. The work at Brookhaven National Laboratory was also supported by the Department of Energy under Contract DE-AC02-76CH00016 (B.M.O.).

References and Notes

(1) Carter, P. W.; Ward, M. D. *J. Am. Chem. Soc.* **1993**, *115*, 11521.
(2) Gavish, M.; Wang, J.-L.; Eisenstein, M.; Lahav, M.; Leiserowitz, L. *Science* **1992**, *256*, 815.
(3) Heywood, B. R.; Mann, S. *J. Am. Chem. Soc.* **1992**, *114*, 4681.
(4) Landau, E. M.; Wolf, S. G.; Levanon, M.; Leiserowitz, L.; Lahav, M.; Sagiv, J. *J. Am. Chem. Soc*. **1989**, *111*, 1436.
(5) Kjaer, K.; Als-Nielsen, J.; Lahav, M.; Leiserowitz, L. In *Neutron and Synchrotron Radiation for Condensed Matter Studies*; Baruchel, J., Hodeau, J.-L., Lehmann, M. S., Regnard, J.-R., Schlekner, C., Eds.; Springer-Verlag: Berlin, 1994; Vol. III, p 47.
(6) Frostman, L. M.; Bader, M. M.; Ward, M. D. *Langmuir* **1994**, *10*, 576.
(7) *Phthalocyanines: Properties and Applications*; Leznoff, C. C., Lever, A. B. P., Eds.; VCH Publishers: New York, 1989; Vol. 1−4.
(8) Cook, M. J. in *Spectroscopy of New Materials*; Advances in Spectroscopy 22; Clark, R. J. H., Hester, H. E., Eds.; John Wiley and Sons: Chichester, 1993; Chapter 3.
(9) Chau, L.-K.; Arbour, C.; Collins, G. E.; Nebesny, K. W.; Lee, P. A.; England, C. D.; Armstrong, N. R.; Parkinson, B. A. *J. Phys. Chem.* **1993**, *97*, 2690.
(10) Chau, L.-K.; England, C. D.; Chen, S.; Armstrong, N. R. *J. Phys. Chem.* **1993**, *97*, 2699.
(11) Palacin, S.; Ruaudel-Teixier, A.; Barraud, A. *J. Phys. Chem.* **1986**, *90*, 6237.
(12) Palacin, S.; Ruaudel-Teixier, A.; Barraud, A. *J. Phys. Chem.* **1989**, *93*, 7195.
(13) Porteu, F.; Palacin, S.; Ruaudel-Teixier, A.; Barraud, A. *J. Phys. Chem.* **1991**, *95*, 7348.
(14) Palacin, S.; Lesieur, P.; Stefanelli, I.; Barraud, A. *Thin Solid Films* **1988**, *159*, 83.
(15) Palacin, S. *Thin Solid Films* **1989**, *178*, 327.
(16) Kroon, J. M.; Sudhölter, E. J. R.; Schenning, A. P. H. J.; Nolte, R. J. M. *Langmuir* **1995**, *11*, 214.
(17) Chou, H.; Chen, C.-T.; Stork, K. F.; Bohn, P. W.; Suslick, K. S. *J. Phys. Chem.* **1994**, *98*, 383.
(18) Gregory, B. W.; Vaknin, D.; Gray, J. D.; Ocko, B. M.; Stroeve, P.; Cotton, T. M.; Struve, W. S. *J. Phys. Chem.* **1997**, *101*, 2006.
(19) Gregory, B. W.; Vaknin, D.; Cotton, T. M.; Struve, W. S. *Thin Solid Films* **1996**, *284/285*, 849.
(20) Palacin, S.; Barraud, A. *J. Chem. Soc., Chem. Commun.* **1989**, 45.
(21) Loschek, R.; Möbius, D. *J. Chim. Phys.* **1988**, *85*, 1041.
(22) Lefevre, D.; Porteu, F.; Balog, P.; Roulliay, M.; Zalczer, G.; Palacin, S. *Langmuir* **1993**, *9*, 150.
(23) Nakashima, N.; Tsuge, A.; Kunitake, T. *J. Chem. Soc., Chem. Commun.* **1985**, 41.
(24) Kirstein, S.; Möhwald, H.; Shimomura, M. *Chem. Phys. Lett.* **1989**, *154*, 303.
(25) Kirstein, S.; Möhwald, H. *Chem. Phys. Lett.* **1992**, *189*, 408.
(26) Kirstein, S.; Steitz, R.; Garbella, R.; Möhwald, H. *J. Chem. Phys.* **1995**, *103*, 818.
(27) Kirstein, S.; Möhwald, H. *J. Chem. Phys.* **1995**, *103*, 826.
(28) Bliznyuk, V.; Möhwald, H. *Thin Solid Films* **1995**, *261*, 275.
(29) Schmitt, F.; Knoll, W. *Chem. Phys. Lett.* **1990**, *165*, 54.
(30) Saito, K.; Ikegami, K.; Kuroda, S.; Tabe, Y.; Sugi, M. *J. Appl. Phys.* **1992**, *71*, 1401.
(31) Nabetani, A.; Tomioka, A.; Tamaru, H.; Miyano, K. *J. Chem. Phys.* **1995**, *102*, 5109.
(32) Wöhrle, D.; Gitzel, J.; Okura, I.; Aono, S. *J. Chem. Soc., Perkin Trans. 2* **1985**, 1171.
(33) Braslau, A.; Pershan, P. S.; Swislow, G.; Ocko, B. M.; Als-Nielsen, J. *Phys. Rev. B* **1988**, *38*, 2457.
(34) Als-Nielsen, J.; Kjaer, K. *Nato Adv. Study Inst. Ser., Ser. B* **1989**, *211*, 113.
(35) Kjaer, K.; Als-Nielsen, J.; Helm, C. A.; Tippman-Krayer, P.; Möhwald, H. *J. Phys. Chem.* **1989**, *93*, 3200.
(36) This is in accordance with the reflectivity model presented previously; see Figure 6 in ref 18 for DHDP on pure water at $A_{DHDP} = 90$ Å^2.
(37) No splitting or additional reflections that usually indicate a distorted hexagonal symmetry were observed at any finite Q_z. However, the line width of the reflection indicates a short correlation length most likely due to incoherent distortions of the hexagonal symmetry.
(38) Kobayashi, T.; Fujiyoshi, Y.; Iwatsu, F.; Uyeda, N. *Acta Crystallogr.* **1981**, *A37*, 692.
(39) Kobayashi, T.; Fujiyoshi, Y.; Uyeda, N. *Acta Crystallogr.* **1982**, *A38*, 356.
(40) Buchholz, J. C.; Somorjai, G. A. *J. Chem. Phys.* **1977**, *66*, 573.
(41) Grand, J.-Y.; Kunstmann, T.; Hoffmann, D.; Haas, A.; Dietsche, M.; Seifritz, J.; Möller, R. *Surf. Sci.* **1996**, *366*, 403.
(42) Collins, G. E.; Williams, V. S.; Chau, L.-K.; Nebesny, K. W.; England, C.; Lee, P. A.; Lowe, T.; Fernando, Q.; Armstrong, N. R. *Synth. Met.* **1993**, *54*, 351.
(43) Vineyard, G. *Phys. Rev. B* **1982**, *26*, 4146.
(44) Martín, M. T.; Prieto, I.; Camacho, L.; Möbius, D. *Langmuir* **1996**, *12*, 6554.
(45) Prieto, I.; Martín Romero, M. T.; Camacho, L.; Möbius, D. *Langmuir* **1998**, *14*, 4175.